04.1

Two types of plasma channel structure in high pressure pulse discharge in cesium

© F.G. Baksht[1], V.F. Lapshin[1,2]

[1] Ioffe Institute, St. Petersburg, Russia
[2] Emperor Alexander I St. Petersburg State Transport University, St. Petersburg, Russia
E-mail: lapshinvf@mail.ru

Received July 23, 2021
Revised July 23, 2021
Accepted August 14, 2021

Simulation of the pulse-periodic high pressure cesium discharge is performed on the basis of equations of radiative gas dynamics. It is shown that in the discharge it is possible to implement two different types of structure of the plasma channel. At the beginning of the current pulse, the plasma discharge channel has a centered structure. At the same time, most of the plasma is concentrated near the discharge axis. The concentration of charged particles decreases along the radius.Then, if the current amplitude is large enough, during the plasma heating process, a transformation from the centered to the shell structure of the channel occurs. In this case, most of the plasma is concentrated on the periphery of the discharge and its concentration increases along the radius from the axis to the walls of the tube. It is shown that the transition from one channel structure to another occurs at a time when the specific heat capacity of the plasma near the axis reaches a deep minimum corresponding to a completely single ionized $e-i$-plasma.

Keywords: low-temperature plasma, pulse discharge, plasma channel.

DOI: 10.21883/TPL.2022.14.55125.18972

A high-pressure pulse gas discharge bounded by solid walls is used widely to produce efficient and intense sources of ultraviolet, visible, and infrared radiation. Regimes with a plasma channel assuming the simplest centered structure (when plasma is concentrated mostly in the near-axial region) have been examined in earlier studies into such discharges [1–5]. Recent research [6–9] indicates that the plasma channel in a high-pressure pulse-periodic discharge (PPD) in cesium may assume different forms. In the present study, a PPD in cesium is used as an example to examine the transformation of the plasma discharge channel from a centered structure to a shell one in the process of plasma heating by a current pulse.

A long ceramic Al_2O_3 discharge tube with inner radius $R = 2\,\text{mm}$ is modeled. The steady-state regime with a current pulse of predetermined amplitude $I_{\max} = 100\,\text{A}$ and duration $t_p = 50\,\mu\text{s}$ passing periodically (with frequency $\nu = 1400\,\text{Hz}$) through plasma of the „routine“ discharge sustained by DC current $I_0 = 1.0\,\text{A}$ is examined. The amount of cesium in the tube is defined by saturated vapor pressure p_{sat} in the coldest end of the tube. At $p_{sat} = 75-500\,\text{Torr}$, the pulse plasma pressure reaches a value of $p = 400-1200\,\text{Torr}$, the wall temperature of the gas-discharge tube is $T_w = 1300-1500\,\text{K}$, and the on-axis plasma temperature is as high as 17 000 K. Plasma with these parameters is in local thermodynamic equilibrium, and the Saha–Boltzmann equations are applicable to it. The equations of radiative gas dynamics written with account for the substantially subsonic velocities of plasma motion and the discharge symmetry are used to model a PPD in cesium:

$$\frac{\partial}{\partial t}(n_a + n_i) + \frac{1}{r}\frac{\partial}{\partial r}\left[r(n_a V_a + n_i V_i)\right] = 0, \quad (1)$$

$$n_e n_1 = K_1(T) n_a,\ n_e n_2 = K_2(T) n_1,\ n_e n_3 = K_3(T) n_2, \quad (2)$$

$$\frac{\partial}{\partial r} p_a = n_a n_1 (V_i - V_a) r_{ai}, \quad (3)$$

$$\frac{\partial}{\partial r}(p_e + p_i) = n_1 n_a (V_a - V_i) r_{ai}, \quad (4)$$

$$\frac{\partial}{\partial t}\left[\frac{3}{2}(n_a + n_i + n_e) k_{\text{B}} T + n_a E_a + n_i E_i\right] + \frac{1}{r}\frac{\partial}{\partial r}\left\{r\left[\frac{5}{2} k_{\text{B}} T (n_e V_e + n_a V_a + n_i V_i) + E_a n_a V_a + E_i n_i V_i\right]\right\} = \sigma E^2 + \frac{1}{r}\frac{\partial}{\partial r} r\lambda \frac{\partial T}{\partial r} - W_{rad}, \quad (5)$$

$$I(t) = 2\pi E_z(t) \int_0^R r \sigma_e(r, t) dr. \quad (6)$$

Here, r is the radial coordinate; k_{B} is the Boltzmann constant; T is temperature; n_α, V_α, and $p_\alpha = n_\alpha k_{\text{B}} T$ are the concentration, the radial velocity, and the partial pressure, respectively, of plasma component α ($\alpha = a, i, e$); n_1, n_2, and n_3 are the concentrations of singly, doubly, and triply ionized cesium atoms; $n_e = n_1 + 2n_2 + 3n_3$; $n_i = n_1 + n_2 + n_3$; E_a is the excitation energy of atoms averaged over the Boltzmann distribution; $n_i E_i = n_1 E_1 + n_2(E_1 + E_2) + n_3(E_1 + E_2 + E_3)$; $E_1 = 3.89\,\text{eV}$, $E_2 = 23.15\,\text{eV}$, and $E_3 = 33.4\,\text{eV}$ are the

energies of the first, the second, and the third ionization of cesium atoms [10]; E_z is the intensity of the longitudinal electric field in plasma; and $K_1(T)$, $K_2(T)$, and $K_3(T)$ are the equilibrium constants from the Saha relation [11,12]. The procedure outlined in [3] was used to calculate the coefficients of electric conductivity σ_e, thermal conductivity λ, and friction r_{ai} for partially ionized plasma. The expressions for λ and σ_e from [13] were used in the case of fully ionized plasma containing ions of various multiplicity.

It is assumed that the radial current to the gas-discharge tube walls is zero and the radial velocities of electrons and all types of ions are the same ($V_i = V_e$). A low-current discharge, where the effect of self-constriction by the intrinsic magnetic field is negligible, is considered.

The values of radiative plasma energy losses W_{rad} were calculated by direct integration of the radiative transfer equation [14]. Absorption coefficient k_λ, which corresponds to the processes of photoionization of excited states of cesium ions, was calculated in the hydrogen-like approximation [11]. The method from [3] was used to calculate k_λ in all other cases.

The boundary conditions for Eqs. (1)–(6) at $r = 0$ correspond to the condition of axial plasma symmetry. The boundary conditions at the tube wall are written with account for the fact that cesium mass M per a unit tube length in the steady-state PPD regime remains constant throughout the entire current pulse period:

$$M = 2\pi m_a \int_0^R r(n_a + n_i)dr = \text{const}. \qquad (7)$$

Here, m_a is the cesium atom mass. Plasma temperature $T(R)$ is assumed to be equal to tube wall temperature T_w and is specified by relation [6]:

$$T(R) = T_w = \left(\frac{q_{pl} + q_{rad}}{\varepsilon_w \sigma_{\text{SB}}(1 + \Delta R/R)}\right)^{1/4} + \frac{R}{\lambda_w}\ln\left(1 + \frac{\Delta R}{R}\right)(q_{pl} + a q_{rad}). \qquad (8)$$

Here, ΔR is the wall thickness ($\Delta R = 1.5$ mm was set in calculations); $\lambda_w = 13\,\text{W}\cdot\text{m}^{-1}\cdot\text{K}^{-1}$ and $\varepsilon_w = 0.3$ are the thermal conductivity and the total emissivity of sapphire [15]; σ_{SB} is the Stefan–Boltzmann constant; $a = 0.5[1/\ln(1+\delta) - 1/(\delta + 0.5\delta^2)]$; $\delta = \Delta R/R$; $q_{pl} = -\nu \int_0^{t_{per}} \left(\lambda \frac{\partial T}{\partial r}\right)\Big|_{r=R} dt$ is the period-average heat flux from plasma to the inner wall surface of the gas-discharge tube due to thermal conductivity; and $t_{per} = 1/\nu$, q_{rad} is the period-average radiation energy flux absorbed by the gas-discharge tube walls [6].

The results of simulation of a PPD in cesium performed in accordance with (1)–(8) are presented for two cesium pressures: $p_{sat} = 500$ Torr (Figs. 1, *a*–3, *a*) and 75 Torr (Figs. 1, *b*–3, *b*). These values correspond to cesium masses $M = 0.06$ and $0.009\,\text{mg}\cdot\text{cm}^{-1}$ per a unit tube length. Relation $c_p = (\partial H/\partial T)_{p=\text{const}}$, where $H = (2.5p + n_a E_a + n_i E_i)/\rho$ is the specific enthalpy and $\rho = m_a(n_a + n_i)$ is the plasma density, was used to calculate specific thermal capacity c_p of plasma. Just as W_{rad}, radiative energy losses $W_{vis}(r, t)$ in the visible range ($\lambda = 400$–700 nm) were calculated using the method from [14].

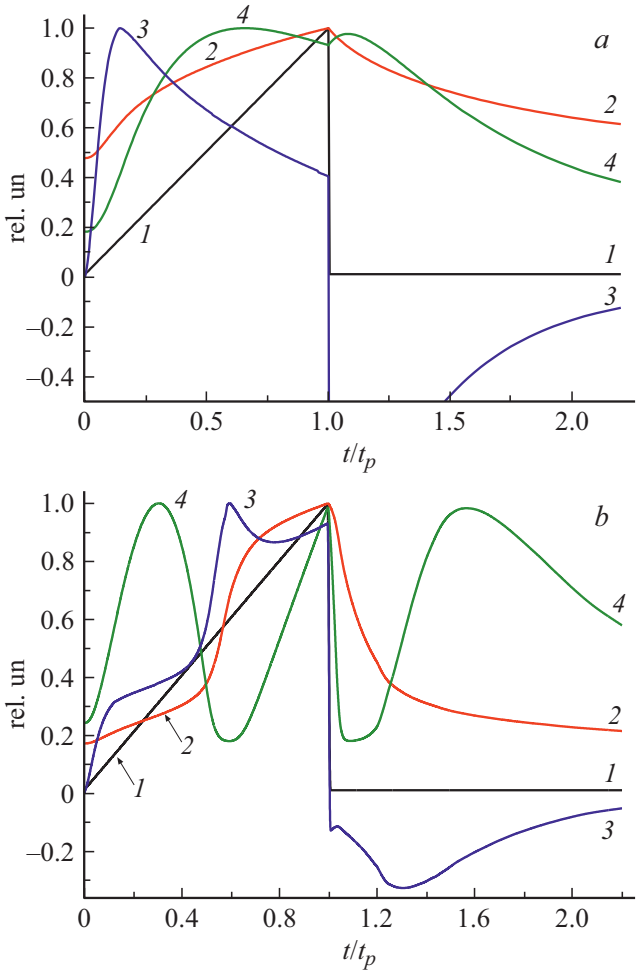

Figure 1. Shape of current pulse $I(t)$ and time dependences of temperature $T_0(t)$, heating power $Q(t)$, and thermal capacity $c_p(t)$ on the discharge axis. *1* — $I(t)/I_{\max}$, *2* — $T_0(t)/T_{0\,\max}$, *3* — $Q(t)/Q_{\max}$, and *4* — $c_p(t)/c_{p\,\max}$. *a* — $p_{sat} = 500$ Torr, $T_{0\,\max} = 6000$ K, $Q_{\max} = 21\,940\,\text{W}\cdot\text{cm}^{-3}$, and $c_{p\,\max} = 1391\,\text{J}\cdot\text{kg}^{-1}\cdot\text{K}^{-1}$; *b* — $p_{sat} = 75$ Torr, $T_{0\,\max} = 17\,610$ K, $Q_{\max} = 17\,980\,\text{W}\cdot\text{cm}^{-3}$, and $c_{p\,\max} = 1778\,\text{J}\cdot\text{kg}^{-1}\cdot\text{K}^{-1}$.

It can be seen from Fig. 1, *a*, temperature T_0 and thermal capacity c_p of plasma on the discharge axis increases smoothly in the course of a pulse if the initial pressure is sufficiently high. A centered structure of the plasma channel (Fig. 2, *a*) is established in this case, and visible radiation is emitted mostly from the near-axis region (Fig. 3, *a*). If the pressure before the onset of a pulse is not that high (Fig. 1, *b*), T_0 grows faster, and there comes a point when almost all gas atoms near the discharge axis

are singly ionized, while the second ionization and ion excitation still remain insignificant. Note that this state is established due to the large difference between energies of the first and the second ionization of alkali metal atoms. Thermal capacity c_p of plasma on the discharge axis decreases sharply in this case, while the value of $Q = \sigma E^2 - W_{rad}$, which specifies the plasma heating power, increases (Fig. 1, *b*, $t/t_p = 0.6$). This leads to a rapid growth of temperature in the near-axis region and expulsion of plasma to the cooler peripheral region (Fig. 2, *b*). A shell structure of the plasma channel with plasma being concentrated mostly at the periphery of the discharge forms as a result. Visible radiation is then emitted mostly from the dense outer shell of the channel (Fig. 3, *b*). The transition from a centered channel structure to a shell one is accompanied by a sharp reduction in the radius of the glowing discharge channel (see [7,9]). Note that the value of c_p in the near-axis region does again go through a deep minimum in the process of plasma cooling after the propagation of a current pulse, and the spatial distribution of plasma in the channel undergoes a reverse transformation.

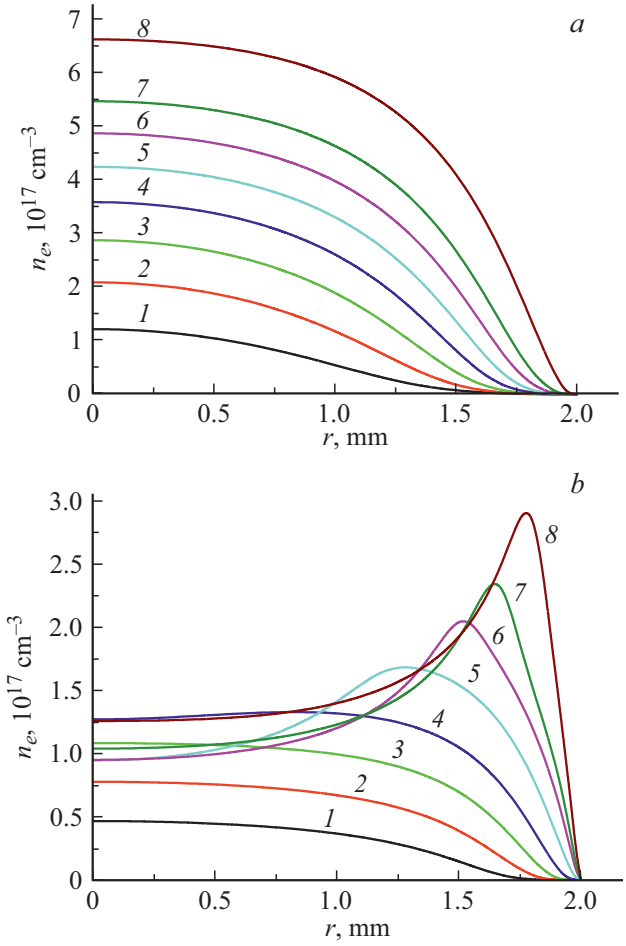

Figure 2. Radial profiles of electron concentration $n_e(r, t)$ at different times t from the onset of a current pulse. t, μs: *1* — 10, *2* — 15, *3* — 20, *4* — 25, *5* — 30, *6* — 35, *7* — 40, and *8* — 50. p_{sat} = 500 (*a*) and 75 Torr (*b*).

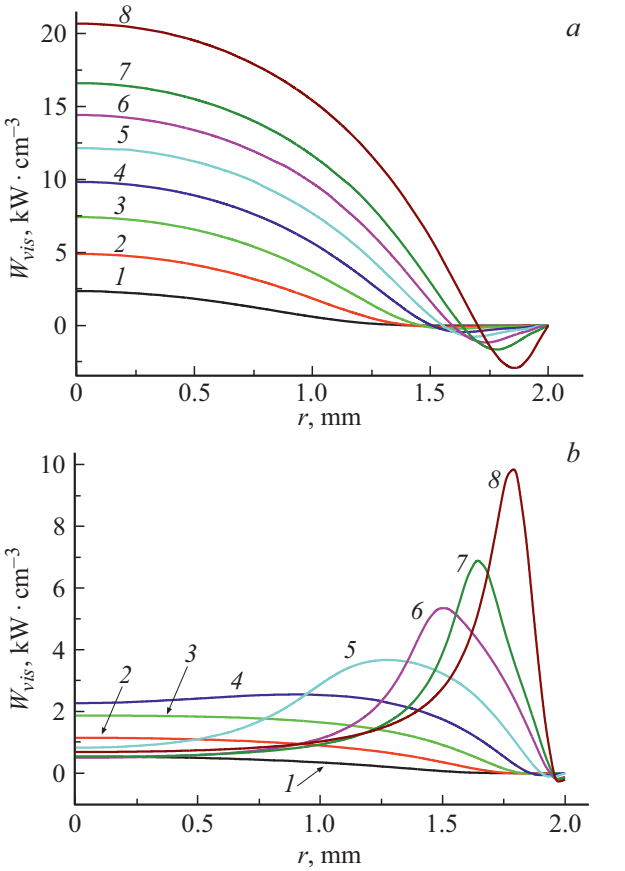

Figure 3. Radial distribution of radiative energy losses $W_{vis}(r, t)$ in the visible range at different times t from the onset of a current pulse. t, μs: *1* — 10, *2* — 15, *3* — 20, *4* — 25, *5* — 30, *6* — 35, *7* — 40, and *8* — 50. p_{sat} = 500 (*a*) and 75 Torr (*b*).

Thus, centered or shell structures of the plasma channel may be established in a pulse-periodic discharge in cesium depending on the initial pressure and the current pulse amplitude. The transformation of one structure into the other one occurs at the moment when the thermal capacity of plasma goes through a deep minimum that corresponds to fully singly ionized $e-i$ plasma.

Conflict of interest

The authors declare that they have no conflict of interest.

References

[1] Yu.S. Protasov, *Entsiklopediya nizkotemperaturnoi plazmy*, Ed. by V.E. Fortov (Nauka, M., 2000), Vol. IV, pp. 232–262 (in Russian).

[2] A.A. Rukhadze, A.F. Aleksandrov, *Fizika sil'notochnykh elektrorazryadnykh istochnikov sveta* (LIBROKOM, M., 2012), pp. 81–89 (in Russian).

[3] F.G. Baksht, V.F. Lapshin, J. Phys. D: Appl. Phys., **41** (20) 205201 (2008). DOI: 10.1088/0022-3727/41/20/205201

[4] M. Rakić, G. Pichler, JQSRT, **151**, 169 (2015). DOI: 10.1016/j.jqsrt.2014.09.022
[5] S.V. Gavrish, V.B. Kaplan, A.M. Martsinovskii, I.I. Stolyarov, Tech. Phys. Lett., **41** (7), 694 (2015). DOI: 10.1134/S1063785015070196.
[6] F.G. Baksht, V.F. Lapshin, Plasma Phys. Rep., **46** (8), 846 (2020).
[7] S.V. Gavrish, V.B. Kaplan, A.M. Martsinovsky, I.I. Stolyarov, Prikl. Fiz., No. 5, 78 (2019) (in Russian).
[8] F.G. Baksht, V.F. Lapshin, Prikl. Fiz., No. 6, 10 (2020) (in Russian).
[9] A.A. Bogdanov, S.V. Gavrish, V.V. Koval', A.M. Martsinovsky, I.I. Stolyarov, Plasma Phys. Rep., **47** (6), 627 (2021).
[10] A.A. Radtsig, B.M. Smirnov, *Parametry atomov i atomnykh ionov: Spravochnik* (Energoatomizdat, M., 1986), p. 109 (in Russian).
[11] V.N. Ochkin, *Spektroskopiya nizkotemperaturnoi plazmy* (Fizmatlit, M., 2010), pp. 20–21, 60–68 (in Russian).
[12] V.E. Fortov, A.G. Khrapak, I.T. Yakubov, *Fizika neideal'noi plazmy* (Fizmatlit, M., 2004), pp. 137–138 (in Russian).
[13] V.M. Zhdanov, *Protsessy perenosa v mnogokomponentnoi plazme* (Fizmatlit, M., 2009), pp. 177–178 (in Russian).
[14] V.F. Lapshin, J. Phys.: Conf. Ser., **669** (1), 012035 (2016). DOI: 10.1088/1742-6596/669/1/012035
[15] G.C. Wei, J. Phys. D: Appl. Phys., **38** (17), 3057 (2005). DOI: 10.1088/0022-3727/38/17/S07